Development 140, 2422-2433 (2013) doi:10.1242/dev.094227

Tbx2/3 is an essential mediator within the Brachyury gene network during *Ciona* notochord development

Diana S. José-Edwards, Izumi Oda-Ishii, Yutaka Nibu*,‡ and Anna Di Gregorio*,‡

SUMMARY

T-box genes are potent regulators of mesoderm development in many metazoans. In chordate embryos, the T-box transcription factor Brachyury (Bra) is required for specification and differentiation of the notochord. In some chordates, including the ascidian *Ciona*, members of the *Tbx2* subfamily of T-box genes are also expressed in this tissue; however, their regulatory relationships with Bra and their contributions to the development of the notochord remain uncharacterized. We determined that the notochord expression of *Ciona Tbx2/3* (*Ci-Tbx2/3*) requires *Ci-Bra*, and identified a *Ci-Tbx2/3* notochord CRM that necessitates multiple Ci-Bra binding sites for its activity. Expression of mutant forms of Ci-Tbx2/3 in the developing notochord revealed a role for this transcription factor primarily in convergent extension. Through microarray screens, we uncovered numerous Ci-Tbx2/3 targets, some of which overlap with known Ci-Bra-downstream notochord genes. Among the Ci-Tbx2/3 notochord targets are evolutionarily conserved genes, including caspases, lineage-specific genes, such as *Noto4*, and newly identified genes, such as *MLKL*. This work sheds light on a large section of the notochord regulatory circuitry controlled by T-box factors, and reveals new components of the complement of genes required for the proper formation of this structure.

KEY WORDS: *Ciona*, Brachyury, Notochord

INTRODUCTION

T-box (or Tbx) genes comprise an evolutionarily conserved class of transcription factors defined by the presence of a distinctive DNA-binding domain. Members of the Tbx family are crucial regulators of embryogenesis (Naiche et al., 2005), and mutations in T-box genes are linked to several human genetic diseases (Packham and Brook, 2003), further underscoring the importance of Tbx transcription factors.

The discovery and functional characterization of *Brachyury* (*Bra*), the founding Tbx family member, revealed its involvement in the specification and development of the notochord (Herrmann et al., 1990). The notochord, the defining feature of chordates, provides structural support for developing embryos throughout this phylum (Jiang and Smith, 2007); a basement membrane and a peri-notochordal sheath consisting of extracellular matrix (ECM) proteins contribute to its rigidity (Stemple, 2005). Elongation of the chordate body plan is in part accomplished through convergent extension (CE) of notochord cells via mediolateral intercalation (Keller et al., 2000), which requires cells to become motile and polarized, to remodel cell-adhesive contacts and to interact with ECM components. Following intercalation, pressure exerted on the notochordal sheath by the formation and expansion of vacuoles provides the tail with further rigidity (Stemple, 2005). Studies in all chordates examined thus far have shown that *Bra* is indispensible for notochord fate commitment (Showell et al., 2004). Conversely, few studies have addressed the composition and regulation of the battery of genes required for later notochord morphogenetic events.

Department of Cell and Developmental Biology, Weill Medical College of Cornell University, 1300 York Avenue, Box 60, New York, NY 10065, USA.

*These authors contributed equally to this work
‡Authors for correspondence (yun2001@med.cornell.edu; and2015@med.cornell.edu)

Accepted 8 April 2013

In addition to the group containing *Bra*, phylogenetic analyses have categorized vertebrate T-box genes into four further subfamilies, including that of *Tbx2*, which in mammals has four members, *Tbx2*, *Tbx3*, *Tbx4* and *Tbx5* (Naiche et al., 2005). The paralogs *Tbx2* and *Tbx3* are important regulators of heart formation (Harrelson et al., 2004), brain morphogenesis (Manning et al., 2006) and cell migration (Fong et al., 2005). In humans, altered levels of these genes have deleterious results: haploinsufficiency caused by mutations in *TBX3* plays a role in ulnar-mammary syndrome (UMS) (Packham and Brook, 2003), and recently *TBX2* and *TBX3* have been found to be amplified or upregulated in different cancers (Lu et al., 2010). These transcriptional regulators can contribute to tumorigenesis through inhibition of apoptosis and by increasing invasiveness through control of cell adhesion genes (Lu et al., 2010). A thorough understanding of the contributions of *Tbx2/3* genes to normal development will thus inform studies of these transcription factors in pathological processes.

Previous studies have suggested that Tbx2 subfamily members could also contribute to notochord formation. *Xenopus* and zebrafish notochords both express *tbx3*, and the zebrafish *tbx2b* gene is also found in the notochord (Dheen et al., 1999; Takabatake et al., 2000); however, their individual functions and regulatory interactions in this tissue remain incompletely characterized. Impaired Tbx2b activity results in defects in notochord specification, which precludes the study of its involvement in later stages of notochord morphogenesis (Dheen et al., 1999; Fong et al., 2005). Hence, the roles and targets of *tbx2* and *tbx3* genes in the development of this structure have yet to be investigated in any chordate.

We have addressed this point using the ascidian *Ciona intestinalis*, a powerful model organism for studies of gene regulation and function during notochord morphogenesis. The ascidian notochord is tractable, consisting of only 40 post-mitotic cells where *Ciona Brachyury* (*Ci-Bra*) is exclusively expressed (Corbo et al., 1997; Passamaneck and Di Gregorio, 2005). *Ciona*

notochord cells intercalate through cellular and molecular mechanisms similar to those used by vertebrates (Jiang et al., 2005; Munro and Odell, 2002b), and require an intact extracellular matrix (Veeman et al., 2008). Formation of intercellular lumens similar to vacuoles also contributes to notochord elongation (Dong et al., 2009; Miyamoto and Crowther, 1985).

Ascidians diverged from the main chordate lineage before the genome duplications associated with the emergence of vertebrates; accordingly, and due to the loss of the ancestral *Tbx4/5* ortholog (Horton et al., 2008), the *Ciona* genome contains only a single *Tbx2* subfamily member, *Ci-Tbx2/3* (Takatori et al., 2004). Among other territories, *Ci-Tbx2/3* is expressed in the notochord after its fate specification, making *Ci-Tbx2/3* both an ideal candidate regulator of notochord differentiation and the only other Tbx gene besides *Ci-Bra* with detectable expression in this tissue. As previous work in *Ciona* has uncovered numerous Ci-Bra downstream genes (e.g. Kugler et al., 2008; Takahashi et al., 1999), the identification of shared Ci-Bra and Ci-Tbx2/3 targets, and the elucidation of the notochord gene regulatory circuitry powered by these transcription factors, are greatly facilitated.

In this study, we focused on the transcriptional regulation and developmental role of *Ci-Tbx2/3* in the *Ciona* notochord. We have analyzed the relationship between *Ci-Tbx2/3* and *Ci-Bra*, and studied the effects of alterations in Ci-Tbx2/3 function on different stages of notochord development, including mediolateral intercalation and lumen formation. Finally, expression profiling identified several Ci-Tbx2/3-dependent notochord genes with various functions, including genes previously reported as Ci-Bra targets. These results shed light on an extensive, crucial branch of the notochord gene regulatory network, components of which appear to be shared between ascidians and higher chordates.

MATERIALS AND METHODS

Embryo culture, electroporation and morpholino injections

Adult *Ciona intestinalis* were purchased from M-REP (Carlsbad, CA). Culturing, electroporations and X-gal staining were carried out as previously described (Oda-Ishii and Di Gregorio, 2007). *Ci-Bra* mutant embryos were kindly provided by Drs Shota Chiba and William Smith (UC Santa Barbara, CA, USA).

The *Ci-Tbx2/3* morpholino (30 fmol), 5′-CGCTATCGGTCAAACACATTCAGAG-3′ (Gene Tools), was co-injected into unfertilized eggs with ~1 μg *Ci-Bra>lacZ* (Corbo et al., 1997). The Ci-Tbx2/3 shRNA plasmid was constructed as described previously (Nishiyama and Fujiwara, 2008) using the oligonucleotides listed in supplementary material Table S2.

Whole-mount *in situ* hybridization

Whole-mount *in situ* hybridizations using BCIP/NBT detection were carried out as previously described (José-Edwards et al., 2011). The *Ci-Tbx2/3* cDNA was constructed by PCR amplifying two overlapping halves of its coding region from cDNA with the primers listed in supplementary material Table S2, then digested and ligated into the pCR4-TOPO vector (Invitrogen). EST clones used for whole-mount *in situ* hybridization were prepared as described previously (José-Edwards et al., 2011); other select cDNAs (supplementary material Table S3) were cloned into the pGEM-T (Promega) vector.

Double-fluorescent whole-mount *in situ* hybridization and immunostaining experiments were performed as described previously (Wagner and Levine, 2012). Anti-DIG-POD (Roche) and rabbit anti-GFP (Invitrogen) antibodies were used at 1:500 and 1:1000 dilutions, respectively. Antisense DIG-labeled probes were visualized through incubation with rhodamine-tyramide working solution (Perkin Elmer) for 5 minutes to 1 hour at room temperature. Embryos were then blocked for 1 hour in TNBS [100 mM Tris (pH 7.5), 150 mM NaCl, 0.5% Roche blocking reagent, 2% normal goat serum] and incubated overnight at 4°C with 1:500 goat anti-rabbit Alexa Fluor 488 (Invitrogen) secondary antibody.

Plasmid construction

Regions of the *Ci-Tbx2/3* locus were amplified from *Ciona intestinalis* genomic DNA. Subsequent deletions and mutations were made using unique restriction sites or through PCR with the oligonucleotides provided in the supplementary material Table S2. These fragments were cloned into the *lacZ*-containing plasmid pFBΔSP6 (Oda-Ishii and Di Gregorio, 2007).

The Ci-Tbx2/3 DBD was amplified from cDNA employing the primers: 5′-AACCATGGATAACATGGAACTGTGGGAGC-3′ and 5′-CTACTAGTTCCGCTCCCTGAGTCTCG-3′, and used to replace the *Ci-FoxN2/3^{DBD}* fragment within the *Ci-Bra>en::Ci-FoxN2/3^{DBD}::GFP* plasmid (kindly supplied by Dr Yale Passamaneck, Kewalo Marine Laboratory, Hawaii, USA) to create *Ci-Bra>en::Ci-Tbx2/3^{DBD}::GFP*. Excision of engrailed from *Ci-Bra>Ci-Tbx2/3^{DBD}::GFP* generated *Ci-Bra>Ci-Tbx2/3^{DBD}::GFP*, and *Ci-Bra>Ci-Tbx2/3^{DBD}::VP16::GFP* was subsequently constructed by amplifying two copies of the VP16 domain from a 4X-VP16 construct using the primers 5′-TTACTAGTGGATCCGCCCCCCCG-3′ and 5′-TTACTAGTCGGCAACCCACCGTACTC-3′, and inserting the product into the *Ci-Bra>Ci-Tbx2/3^{DBD}::GFP* plasmid.

Immunostaining, microscopy and quantitative analysis

For either direct visualization of fluorescence or immunostaining, embryos were fixed as for whole-mount *in situ* hybridization at room temperature for 30 minutes to 1 hour. Double immunofluorescence experiments were performed using 1:1000 rabbit anti-GFP and mouse anti-β-Gal (Promega) primary antibodies and 1:1000 goat anti-rabbit Alexa Fluor 488 and goat anti-mouse Alexa Fluor 555 (Invitrogen) secondary antibodies. Select embryos were counterstained with 1 U rhodamine-phalloidin (Invitrogen) in 1× PBS/0.2% Triton X-100 for 3 hours at room temperature. All fluorescent samples were mounted in VECTASHIELD with DAPI (Vector Laboratories). Images were obtained with a Leica DMR microscope with the exception of confocal images, which were acquired at the Weill Cornell Medical College Optical Microscopy Core Facility using a Zeiss LSM 510 microscope. Data presented in graphs represent average values with error bars indicating the s.d. garnered from at least three independent experiments. Statistical significance for the phenotypic classes of Ci-Tbx2/3 mutants, when compared with *Ci-Bra>GFP* samples, was determined using a χ^2 test.

Microarray screens

Approximately 100-300 fluorescent embryos expressing the *Ci-Bra>Tbx2/3^{DBD}::GFP*, *Ci-Bra>Tbx2/3^{VP16}::GFP* or *Ci-Bra>GFP* transgenes were manually selected at ~7 hpf and ~10.5 hpf (Hotta et al., 2007). RNA was extracted using the RNeasy micro kit (Qiagen) from three biological replicates for each construct and used to create labeled probes for hybridization to a *Ciona intestinalis* Affymetrix GeneChip (Christiaen et al., 2008) by the Weill Cornell Genomics Resources Core Facility. Results were RMA summarized from raw data (CEL files) and quantile normalized before proceeding with ANOVA to statistically analyze the data (Weill Cornell Epigenomics Core Facility). Probe sets with $P \leq 0.05$ with an absolute fold change cut-off of 2 were considered further. The microarray dataset has been deposited into the NCBI Gene Expression Omnibus (accession number GSE42267).

RESULTS

Ci-Tbx2/3 notochord expression depends upon *Ci-Bra*

In *Ciona*, transcripts for *Ci-Tbx2/3* are found in a number of spatial domains, including the notochord (Fig. 1A) (Imai et al., 2004; Takatori et al., 2004). Unlike in other chordates, such as zebrafish (Dheen et al., 1999; Martin and Kimelman, 2008), *Ci-Bra* and *Ci-Tbx2/3* are the only Tbx genes present in the *Ciona* notochord. This fact both simplified the analysis of the contribution of the T-box gene family to notochord development and provided an ideal system for studying the regulatory interactions between these factors.

Expression of *Ci-Bra* begins at the 64-cell stage, concomitant with notochord fate restriction (Corbo et al., 1997), and precedes expression of *Ci-Tbx2/3*, suggesting that the notochord expression of *Ci-Tbx2/3* could be mediated by Ci-Bra. To assess this, we

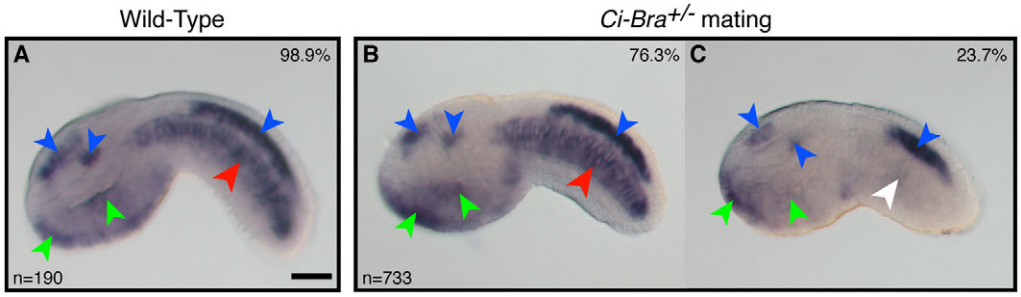

Fig. 1. *Ci-Tbx2/3* notochord expression is controlled by *Ci-Bra*. (**A-C**) Whole-mount *in situ* hybridization for *Ci-Tbx2/3* on mid-tailbud wild-type embryos (A) and the offspring of *Ci-Bra* heterozygous animals (B,C). The percentage of embryos exhibiting each phenotype is provided in the upper right corner of each panel, whereas the total number of embryos scored is in the lower left corner. Notochord expression is highlighted by a red arrowhead, while a white arrowhead denotes lack of expression in this domain. Colored arrowheads indicate other expression domains as follows: blue, CNS; green, epidermis. Scale bar: 40 μm.

analyzed the expression pattern of *Ci-Tbx2/3* in *Ci-Bra*$^{-/-}$ mutant embryos (Chiba et al., 2009). We performed whole-mount *in situ* hybridization for *Ci-Tbx2/3* on the offspring of *Ci-Bra*$^{+/-}$ animals as homozygotes do not survive to adulthood (Chiba et al., 2009). We determined that, compared with controls and wild-type siblings (Fig. 1A,B), *Ci-Tbx2/3* transcripts were not detectable in the notochord of *Ci-Bra*$^{-/-}$ embryos (Fig. 1C), signifying that *Ci-Bra* is indispensable for the expression of *Ci-Tbx2/3* in this domain. In the absence of notochord-specific *Ci-Bra*, *Ci-Tbx2/3* expression in the epidermis and CNS is detected at normal levels, emphasizing that other tissue-specific factors likely activate *Ci-Tbx2/3* in its additional expression domains. Thus, *Ci-Tbx2/3* lies downstream of *Ci-Bra* in the notochord gene regulatory network.

Characterization of a *Ci-Tbx2/3* notochord *cis*-regulatory module (CRM)

The previous results prompted us to investigate in detail the *cis*-regulatory mechanisms mediating the hierarchical interaction between *Ci-Bra* and *Ci-Tbx2/3* in the notochord. Whole-genome VISTA alignments between *Ciona intestinalis* and its sister species *Ciona savignyi* (Frazer et al., 2004) highlighted several stretches of non-coding sequence conservation across the ~15 kb *Ci-Tbx2/3* locus (Fig. 2A). As such areas are often seen as hallmarks of functional *cis*-regulatory DNA, we tested the ability of six genomic fragments encompassing conserved regions within the *Ci-Tbx2/3* locus to direct tissue-specific expression of the *lacZ* reporter *in vivo*. Constructs containing genomic fragments located 5′ of the *Ci-*

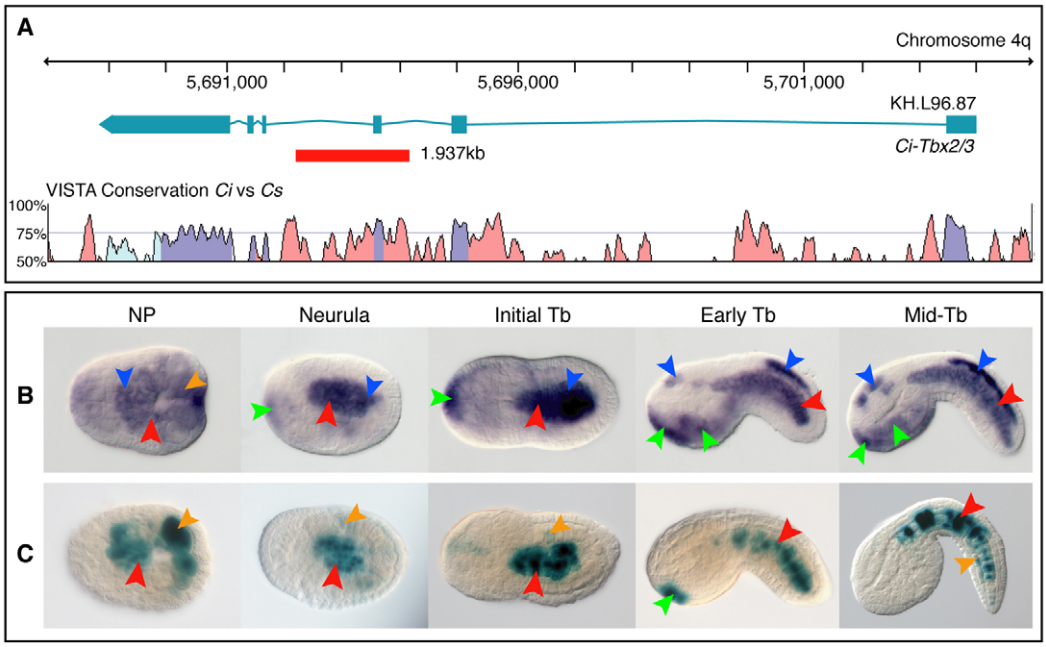

Fig. 2. Identification of a CRM that recapitulates *Ci-Tbx2/3* notochord expression. (**A**) Top: map of the *Ci-Tbx2/3* locus. Exons and introns are denoted by teal rectangles and lines, respectively. A red box indicates the notochord CRM. Bottom: VISTA alignment illustrating the sequence conservation across the *Ci-Tbx2/3* locus between *Ciona intestinalis* (*Ci*) and *Ciona savignyi* (*Cs*), obtained using the following parameters: calculation window, 100 bp; minimum conservation width, 100 bp; conservation identity, 50%. Purple peaks indicate conserved coding regions; light blue peaks indicate conserved 5′- or 3′-UTR; pink peaks indicate conserved non-coding regions. (**B**) *Ci-Tbx2/3* whole-mount *in situ* hybridization. (**C**) X-Gal staining of *C. intestinalis* embryos carrying the *Ci-Tbx2/3* notochord CRM in A. (B,C) Expression territories are highlighted with arrowheads: red, notochord; orange, muscle; blue, CNS; green, epidermis. In most panels, dorsal is upwards and anterior is towards the left. NP, neural plate; Tb, tailbud.

Tbx2/3 transcription start site and within the first intron exhibited staining only in *Ci-Tbx2/3* expression domains outside of the notochord (supplementary material Fig. S1), indicating that the *Ci-Tbx2/3* locus harbors multiple tissue-specific CRMs. Conversely, upon electroporation of a 1.9 kb region spanning part of the second and third introns (Fig. 2A), the resulting embryos displayed robust notochord activity (Fig. 2C), recapitulating the onset and pattern of the endogenous gene in this domain (Fig. 2B). Genome-wide ChIP studies, published after this CRM was identified, showed the highest Ci-Bra binding peaks within the first intron in early (110-cell stage) embryos (Kubo et al., 2010); however, we found that these areas lacked notochord staining (supplementary material Fig. S1). Nonetheless, another peak was contained in the 1.9 kb region with notochord activity, consistent with our results (Kubo et al., 2010).

In order to identify the minimal *cis*-regulatory sequences necessary for the activity of this notochord CRM, we tested the ability of truncations of the 1.9 kb region to retain notochord expression (supplementary material Fig. S2). A 294 bp region drove consistent *lacZ* expression in the notochord and was enriched for T-box binding sites, containing nine sequence blocks (T1-T9) matching the generic TNNCAC Ci-Bra consensus binding site (e.g. Dunn and Di Gregorio, 2009) (Fig. 3A,B), supporting a role for Ci-Bra in the activation of this notochord CRM.

To determine the functional requirements of such sites for notochord activity, we analyzed the 294 bp CRM further. Two overlapping halves of this sequence, 172 bp (T1-T6) and 151 bp (T6-T9), directed weakened notochord expression; however, notochord expression of the 151 bp fragment was lost upon removal of sites T6 and T7 (supplementary material Fig. S2). Given this result, we first mutagenized T6 as it was common to both partially active halves of the CRM. Because mutation of T6 alone did not abolish notochord activity (Fig. 3A,D), we examined the contribution of T5 and T7, the T-box sites adjacent to T6. However, as with T6, we found that obliterating either of those sites individually did not result in a decrease in notochord activity (Fig. 3A,C,E). Rather, we observed an apparent increase in the number of embryos exhibiting notochord staining upon mutation of either T5 or T6. In the wild-type CRM, we observed that notochord staining is often accompanied by ectopic muscle staining (light pink bars in the chart in Fig. 3A). This is likely due to the T-box sites being bound by the muscle-specific T-box factor(s) Tbx6b and/or Tbx6c when the CRM is isolated from its genomic context. Consistently, a peak of Tbx6b occupancy was found in the region corresponding to the 294 bp CRM in early embryos (supplementary material Fig. S1) (Kubo et al., 2010). Muscle cells are large and located more superficially than notochord cells, such that strong muscle staining can mask the notochord activity. When T5 and T6 were mutated, more embryos exhibited notochord-specific expression (maroon bars in the chart in Fig. 3A) because the loss of muscle staining increased the visibility of the notochord.

Because disruptions of single T-box sites did not eliminate *lacZ* notochord expression, we created constructs carrying compound mutations and found that disruption of T6 in combination with either T5 or T7 resulted in a drastic abrogation of notochord activity (Fig. 3A,F,G). Simultaneous disruption of T5 and T7 was less effective, with 6% of embryos still exhibiting notochord staining (Fig. 3A,H), suggesting that the individual T-box sites are mostly, although not completely, redundant. Any residual notochord activity was lost upon simultaneous mutation of T5, T6 and T7 (Fig. 3A,I).

The *Ciona savignyi* region corresponding to the 294 bp notochord CRM also harbors a number of T-box sites, and the notochord activity of the *Ci-Tbx2/3* 294 bp CRM in *C. savignyi* embryos was similar to that in *C. intestinalis* (supplementary material Fig. S3). These results strongly suggest that the *cis*-regulatory strategy that ensures notochord expression of *Ci-Tbx2/3* is evolutionarily conserved between these two species.

Roles of Ci-Tbx2/3 in notochord formation

In prior studies, notochord expression of *Ci-Tbx2/3* was detected starting at neurulation (Imai et al., 2004; Takatori et al., 2004) when

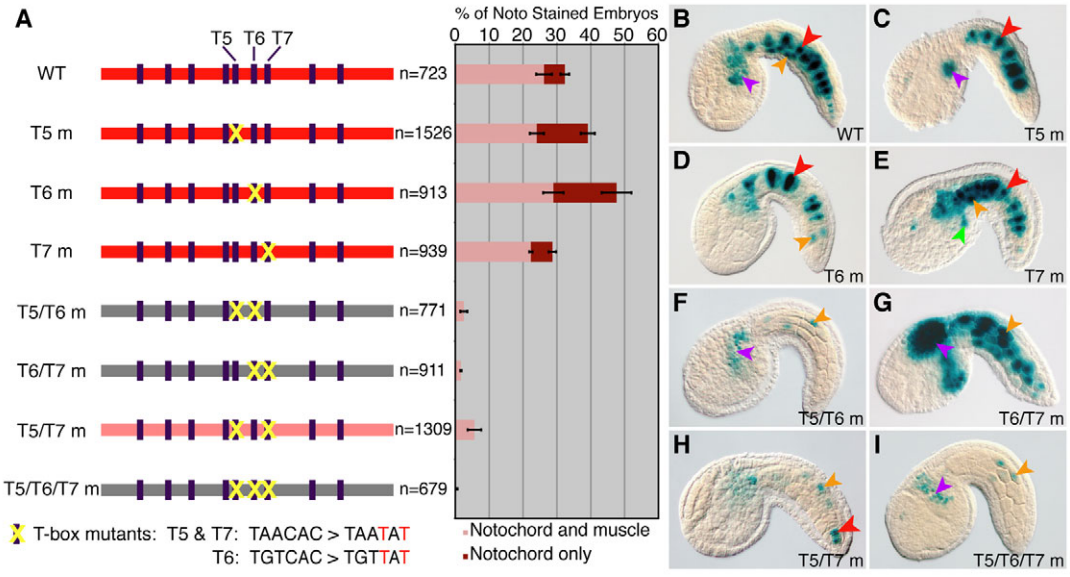

Fig. 3. Activity of the *Ci-Tbx2/3* notochord CRM requires T-box binding sites. (**A**) Left: schematic representation of the 294 bp *Ci-Tbx2/3* notochord CRM. Red boxes represent constructs with notochord activity; configurations exhibiting weak or lack of notochord activity are depicted by light-red and gray boxes, respectively. Dark purple rectangles depict T-box binding sites. Right: percentage of embryos exhibiting notochord staining when electroporated with the wild-type (WT) or T-box (T) mutant plasmids to the left of each bar. (**B-I**) Microphotographs showing X-Gal stained embryos expressing the constructs in A. Arrowheads are colored as follows: red, notochord; orange, muscle; purple, mesenchyme. m, mutant.

intercalation first begins (Munro and Odell, 2002b). However, we observed *Ci-Tbx2/3* notochord expression from the neural plate through tailbud stages (Fig. 2B), suggesting that Ci-Tbx2/3 might contribute to various steps of notochord differentiation, including CE.

To determine whether Ci-Tbx2/3 participates in notochord formation, we disrupted its function using several approaches. Morpholino oligonucleotide (MO) knockdown of *Ci-Tbx2/3* resulted in extensive defects in body axis length and abnormally shaped heads; the shortened, curled tails of morphants (supplementary material Fig. S4A-A″) suggested that the notochord fails to extend and acquire rigidity upon *Ci-Tbx2/3* knockdown. The severity of the MO-induced phenotypes, owing to the expression of *Ci-Tbx2/3* in multiple territories (Fig. 1A), prevented further characterization of notochord-specific defects. To circumvent this limitation, we expressed mutant forms of *Ci-Tbx2/3* in the notochord using the *Ci-Bra* promoter region (Corbo et al., 1997). Because the domain structure of Ci-Tbx2/3 is uncharacterized except for the evolutionarily conserved DNA-binding domain (DBD), we built three versions of Ci-Tbx2/3. We first created a dominant-negative by cloning the DBD downstream of the *Ci-Bra* promoter (*Ci-Tbx2/3*^{DBD}); the resulting protein would be expected to simply bind target genes and neither activate nor repress transcription. We also engineered heterologous fusions of the DBD with the VP16 activation (*Ci-Tbx2/3*^{VP16}) or Engrailed repression (*Ci-Tbx2/3*^{En}) domains (Kugler et al., 2008; Sadowski et al., 1988) to create constitutive activator or repressor forms, respectively. All constructs also encoded GFP to allow for the detection of incorporation of the transgenes.

CE transforms the *Ciona* notochord from a monolayer of 40 notochord cells into a cylindrical rod a single cell in diameter (Munro and Odell, 2002b) (Fig. 4A). When *Ciona* zygotes were electroporated with either the *Ci-Tbx2/3*^{DBD} or the *Ci-Tbx2/3*^{VP16} plasmid, the resulting embryos showed defective intercalation and impaired tail elongation (Fig. 4). Taking into account mosaic incorporation of the transgenes (Di Gregorio and Levine, 2002), which results in variable severity of the phenotype and produces a mixture of transgenic and non-transgenic notochord cells, we grouped the observed phenotypes into four classes: mild (mostly normal, but displaying incomplete intercalation along some points of the tail, Fig. 4B), moderate (two rows of notochord cells, Fig. 4C), severe (more than two rows of notochord cells, Fig. 4D) and very severe (transgenic cells mislocalized to the trunk, Fig. 4E). The incidence of abnormal notochord development was significantly increased in Ci-Tbx2/3^{DBD} and Ci-Tbx2/3^{VP16} embryos (79.8% and 90.7%, respectively) compared with control embryos expressing the neutral *Ci-Bra>GFP* transgene (Corbo et al., 1997) (~33%, Fig. 4F). Despite their abnormalities, Ci-Tbx2/3^{DBD} and Ci-Tbx2/3^{VP16} embryos still contained 40 notochord cells, even though *Ci-Tbx2/3* is expressed prior to the last cell division of notochord precursors (Jiang and Smith, 2007); therefore, Ci-Tbx2/3 appeared not to affect notochord cell mitosis. *Ci-Tbx2/3* shRNA constructs and the *Ci-Tbx2/3*^{En} fusion also produced similar notochord phenotypes (supplementary material Fig. S4); however, the low fluorescence of embryos electroporated with the latter construct prevented its use in further experiments.

As described above, electroporated embryos contained different proportions of transgenic and wild-type notochord cells (Fig. 4G-H′). In controls, notochord cells appeared in single file along the length of the tail, intercalated cells had aligned nuclei, and both GFP-positive and GFP-negative cells were disk-shaped (Fig. 4G,G′;

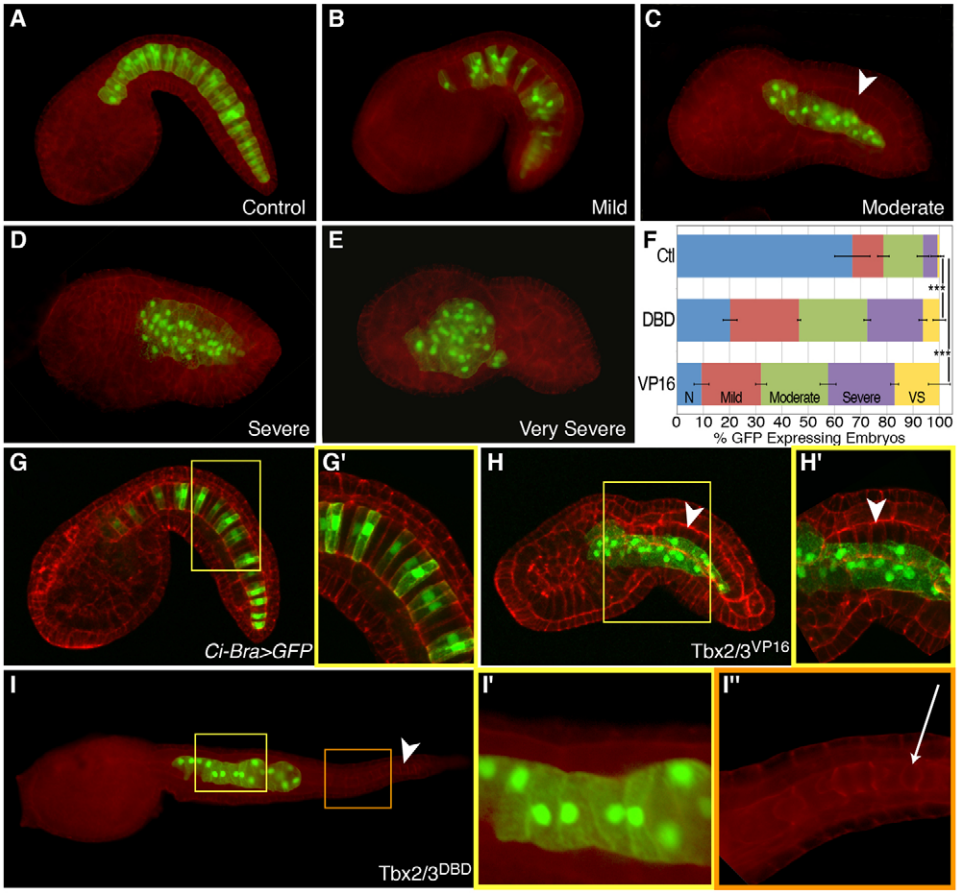

Fig. 4. Perturbation of Ci-Tbx2/3 function causes defects in notochord morphogenesis. (**A**) *Ci-Bra>GFP* control embryo. (**B-E**) Classification of notochord intercalation defects observed in embryos electroporated with either *Ci-Bra>Tbx2/3*^{DBD}*::GFP* or *Ci-Bra>Tbx2/3*^{VP16}*::GFP*. (**F**) Quantification of phenotypic categories displayed in A-E. *n*=1581 for control (Ctl), *n*=586 for DBD and *n*=309 for VP16; N, normal; VS, very severe. ***P<0.001 compared with controls. (**G-H′**) Confocal *z*-stacks of *Ci-Bra>GFP* controls (G,G′) and *Ci-Bra>Tbx2/3*^{VP16}*::GFP* (H,H′) stage-matched embryos. (**I-I″**) Larva (~17.5 hpf) expressing *Ci-Bra>Tbx2/3*^{DBD}*::GFP*. (G′,H′,I′,I″) Higher magnification views of the areas boxed in yellow or orange in G, H and I, respectively. White arrowheads indicate non-transgenic notochord cells, whereas a white arrow (I″) indicates a lumen between non-transgenic cells. All embryos were counterstained with rhodamine-phalloidin (red).

supplementary material Movie 1), characteristic of proper notochord formation. By contrast, no such uniformity was seen in embryos expressing either of the altered forms of Ci-Tbx2/3: the transgenic cells in these animals varied in shape and size, appeared in multiple planes and their nuclei were variably located (Fig. 4H,H′; supplementary material Movie 2). In moderately affected Ci-Tbx2/3^{DBD} and Ci-Tbx2/3^{VP16} embryos, transgenic and non-transgenic notochord cells often appeared spatially separated. For example, in Fig. 4H, fluorescent cells harboring Ci-Tbx2/3^{VP16} are located ventral-laterally of the non-transgenic notochord cells. This segregation is surprising as cells from both sides of the midline mix randomly during notochord intercalation (Miyamoto and Crowther, 1985; Munro and Odell, 2002b) in *Ci-Bra>GFP* control embryos (Fig. 4G,G′). Taken together, this phenomenon, along with the different phenotypic variations observed, suggest that these intercalation defects could be due to dose-dependent deficiencies in the motility of the transgenic notochord cells.

At the final stages of notochord differentiation, the notochord normally begins to turn into a hollow tube through the formation of extracellular lumens (Fig. 4I-I″) (Dong et al., 2009). These structures were absent in *Ci-Tbx2/3^{VP16}*- or *Ci-Tbx2/3^{DBD}*-expressing cells (Fig. 4I′). Overall, therefore, Ci-Tbx2/3 contributes to different stages of notochord differentiation.

We also monitored the development of tissues adjacent to the notochord in transgenic embryos. The CNS activity of the marker CRM *Ci-ETR* (Satou et al., 2001) was unaffected by expression of *Ci-Tbx2/3^{VP16}* (supplementary material Fig. S5A,B); therefore, the phenotype induced by notochord-specific expression of *Ci-Tbx2/3^{VP16}* appeared cell-autonomous. Muscle cells also appeared to be properly specified; however, they failed to elongate along the anterior-posterior axis (supplementary material Fig. S5C,D), consistent with previous observations correlating the elongation of the notochord with the shape of muscle cells (Di Gregorio et al., 2002; Munro and Odell, 2002a).

Differential regulation of target genes by Ci-Tbx2/3

In order to identify candidate Ci-Tbx2/3 target genes, we performed genome-wide microarray analyses on *Ci-Tbx2/3^{DBD}*- and *Ci-Tbx2/3^{VP16}*-expressing embryos. Total RNA was isolated from transgenic embryos and stage-matched *Ci-Bra>GFP* controls at the mid-late neurula and mid-tailbud I/II stages (Hotta et al., 2007), with the aim of capturing targets expressed throughout and following intercalation. These screens yielded 94 probe sets with significant differential expression of at least twofold, corresponding to 81 genes. The datasets obtained from the two stages were mostly non-overlapping, highlighting the dynamic nature of the notochord transcriptome regulated by Ci-Tbx2/3. Furthermore, Ci-Tbx2/3^{DBD} and Ci-Tbx2/3^{VP16} appear predominantly to regulate distinct sets of targets, although the phenotypes induced by these transgenes are similar; this is consistent with a related screen that found that the VP16 domain influenced TBX2 target selection (Butz et al., 2004). Notably, our results also indicate that Ci-Tbx2/3^{VP16} may act as an activator in only a few instances (e.g. for *Nicastrin*); instead, in the majority of cases, this chimera appears to operate as a dominant-negative form because, surprisingly, several genes that emerged from the Ci-Tbx2/3^{VP16} screen were downregulated (e.g. *Noto4,* Table 1).

To validate the microarray results, we performed whole-mount *in situ* hybridization for the 81 candidate targets and observed a detectable signal for 70 genes (Fig. 5A). As expected, the screen identified several notochord genes (20/70, ~29%) (Fig. 5A-H; Table 1; supplementary material Fig. S6), 13 of which are novel, including *fibronectin 1-containing* (*FN1-cont.*), *thrombospondin 1-*

Table 1. Notochord gene targets from microarray screen of embryos expressing *Tbx2/3^{DBD}* or *Tbx2/3^{VP16}*

Gene name	KH gene model*	JGI v1.0 gene model	Data set	Fold change‡	Source of notochord expression pattern
Caspase9-like (Casp9-like)	KH.C3.375	ci0100130387	DBD	–6.32	(Satou et al., 2001)§
Nicastrin	KH.C1.1147	ci0100130440	VP16	6.24	This study (supplementary material Fig. S6A)
Glycoprotein V-like (GPV-like)	KH.C7.584	ci0100154658	VP16¶	–5.28	This study (Fig. 5L)
Uncharacterized Transcript	KH.C1.650	ci0100132205	DBD	5.24	This study (supplementary material Fig. S6B)
Uncharacterized Transcript	KH.C8.749	N/A	VP16¶	–5.11	This study (Fig. 5G)
			DBD	–2.02	
Uncharacterized Transcript	N/A	ci0100144542	DBD	4.68	This study§ (supplementary material Fig. S6C)
Uncharacterized Transcript	KH.C12.600	N/A	VP16¶	–4.19	This study (Fig. 5H)
Slc23a	KH.C7.199	ci0100152342	VP16¶	–4.18	(Kusakabe et al., 2002)§
Duox-c	KH.C2.477	ci0100134721	VP16	4.26	This study§ (Fig. 5N)
			DBD	3.27	
Fibronectin1 (FN1)-containing	KH.C10.317	N/A	VP16¶	–3.10	This study (Fig. 5D)
Chd8/9	KH.C12.278	N/A	DBD	–3.06	(Kusakabe et al., 2002)§
Noto4	KH.L18.30	ci0100138226	VP16¶	–3.00	(Hotta et al., 2000)
MLKL	KH.C4.411	ci0100152391	VP16¶	–2.77	This study (Fig. 5F)
Cytosolic Sulfotransferase (SULT)	KH.C7.721	ci0100133920	VP16¶	–2.48	(Christiaen et al., 2008) (Fig. 5C)
Thrombospondin 1 (Thsd1)-containing	KH.C2.1123	ci0100153405	VP16¶	–2.38	This study (Fig. 5E)
Atlastin	KH.C12.101 KH.C12.437	ci0100131717	DBD	–2.18	This study§ (Fig. 5B)
Ci-META6-like	KH.S655.4	ci0100144948	DBD	2.13	This study (supplementary material Fig. S6D)
Fos-a	KH.C11.314	ci0100130316	DBD	2.04	(José-Edwards et al., 2011)§
Phex	KH.C12.669	ci0100141711	DBD	–2.03	This study§ (supplementary material Fig. S6E)
ZF105	KH.C2.23	ci0100143717	VP16¶	–2.00	(Miwata et al., 2006)

*Satou et al., 2008.
‡Negative and positive scores denote downregulation and upregulation, respectively, compared with Bra>GFP controls.
§Transient (spanning one or two stages) or patchy notochord staining.
¶In these cases Tbx2/3^{VP16} appears to be acting as a dominant-negative (see text).
ZF, zinc-finger; v1.0, version 1.0; N/A, not applicable; DBD, DNA-binding domain (dominant-negative form).

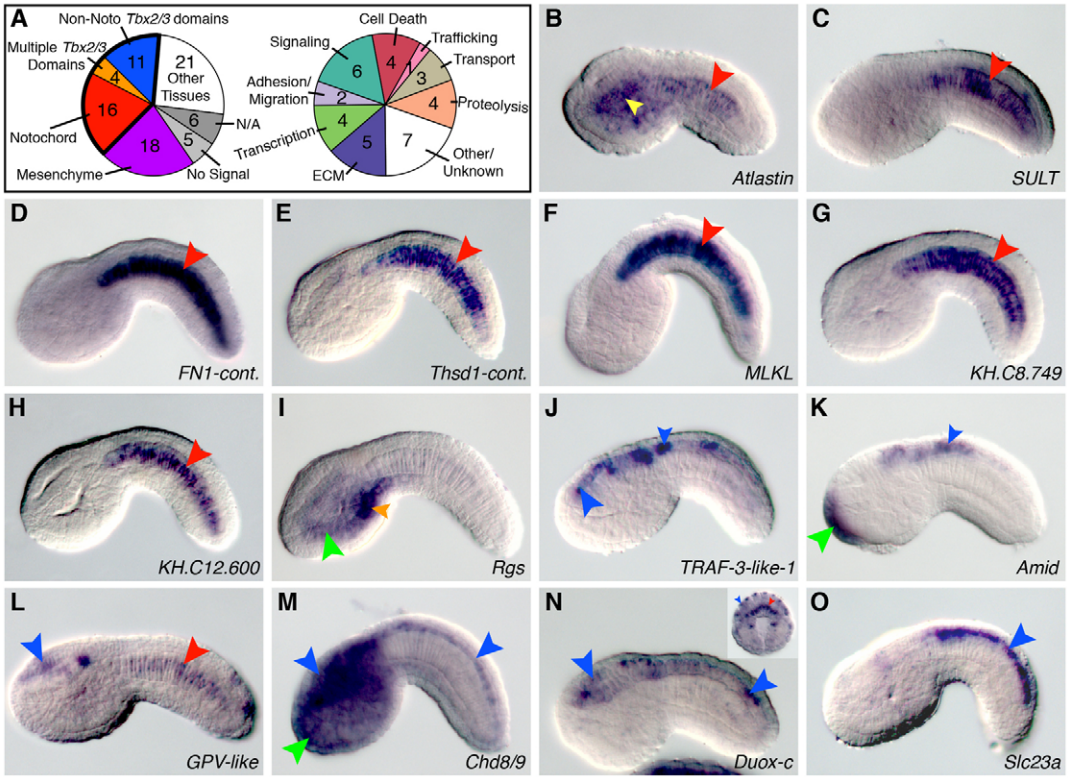

Fig. 5. Expression patterns of candidate Ci-Tbx2/3 targets identified via microarray screen. (**A**) Left: pie chart summarizing the expression patterns of 81 potential Ci-Tbx2/3 target genes. The 'multiple *Tbx2/3* domains' category represents those genes found in the notochord and at least one non-notochord *Ci-Tbx2/3* expression territory. Right: pie chart depicting putative functions for the 31 targets expressed in *Ci-Tbx2/3* expression domains (outlined in bold on the left). Some genes are present in multiple categories. (**B-O**) Whole-mount *in situ* hybridization on early to late tailbud embryos for the genes listed in the lower right corner of each panel. The inset in N shows a 110-cell stage embryo probed for *Duox-c* expression. Stained territories are denoted by colored arrowheads as follows: red, notochord; orange, muscle; blue, CNS; green, epidermis; yellow, endoderm. Larger arrowheads signal expression in domains matching that of *Ci-Tbx2/3*, whereas smaller arrowheads indicate expression in other areas. Cont., containing; N/A, not assayed.

containing (*Thsd1-cont.*) and *mixed linage kinase domain-like* (*MLKL*). The microarray data suggested that Ci-Tbx2/3 serves to activate the notochord expression of these genes, as the majority were downregulated when the function of this transcription factor was impaired (Table 1).

Interestingly, despite the fact that Ci-Tbx2/3^{DBD} and Ci-Tbx2/3^{VP16} were expressed almost exclusively in the notochord, we identified a number of targets (11/70, ~16%) in the CNS and epidermis, other *Ci-Tbx2/3* expression domains (Fig. 5A,I-K; supplementary material Table S1). We observed that these non-notochord targets, including *Rgs* and *claudin gene family member 3*, tend to be upregulated (supplementary material Table S1), implying that they are normally repressed by Ci-Tbx2/3 in the notochord, but activated in the CNS and/or epidermis. In vertebrates, Tbx2 and Tbx3 are thought to act as both activators and repressors (Washkowitz et al., 2012), and the direction of regulation of their targets can vary in a context-dependent manner, such that a gene may be upregulated in one circumstance, but downregulated in another (Butz et al., 2004; Chen et al., 2001; Paxton et al., 2002). The above results, and the fact that we obtained similar phenotypes upon expression of Ci-Tbx2/3^{DBD}, Ci-Tbx2/3^{VP16} and Ci-Tbx2/3^{En} (Fig. 4; supplementary material Fig. S4), suggested that Ci-Tbx2/3 could both activate and repress transcription, similar to its vertebrate counterparts. However, we cannot rule out that Ci-Tbx2/3 may indirectly regulate some of these downstream genes.

A third category of Ci-Tbx2/3 targets was expressed in both the notochord and other Ci-Tbx2/3 expression domains (Fig. 5A,L-O). *Duox-c* was transiently expressed in the notochord in early embryos (110-cell stage), but became restricted to various regions of the CNS at later stages (Fig. 5N). Downregulation of *Duox-c* in the notochord occurs following the neural plate stage (data not shown) when *Ci-Tbx2/3* expression commences in this domain (Fig. 2B), consistent with the hypothesis that Ci-Tbx2/3 might repress transcription. This suggests that Ci-Tbx2/3 may also contribute to the temporal control of notochord expression. Furthermore, *Slc23a* is expressed in the posterior nerve cord at tailbud stages (Fig. 5O), like *Ci-Tbx2/3*, but switches to the notochord in larvae (Kusakabe et al., 2002). This temporal and spatial variability indicates that the function of Ci-Tbx2/3 is likely modified locally by tissue-specific regulators.

Ci-Tbx2/3 controls genes involved in a wide variety of cellular processes

Fig. 5A categorizes the 31 bona fide targets detected in Ci-Tbx2/3 expression territories according to their predicted functions, e.g. cell death, ECM, transcription, adhesion, signaling and others. This suggests that Ci-Tbx2/3 controls a wide array of cellular processes required to develop the notochord, CNS and epidermis properly, and explains the severe developmental defects observed when the function of this transcriptional regulator is manipulated.

The most extensively characterized notochord gene controlled by Ci-Tbx2/3 is *Noto4* (Table 1), a gene originally identified as a transcriptional target of Ci-Bra (Takahashi et al., 1999). Noto4 has been shown to be required for notochord intercalation (Yamada et al., 2011); *Noto4* morphants display intercalation defects evocative of the phenotypes observed in embryos expressing the Ci-Tbx2/3^{DBD} and Ci-Tbx2/3^{VP16} transgenes, strongly suggesting that *Noto4* is one of the main effectors of Ci-Tbx2/3. In addition to *Noto4*, *cytosolic sulfotransferase* (*SULT*) (Fig. 5C) had been previously identified as a positive mediator of cell migration in *Ciona* heart precursors (Christiaen et al., 2008). The downregulation of this gene in Ci-Tbx2/3^{VP16} embryos could contribute to the impairment of notochord cell motility that we observed (Fig. 4).

Among the developmental regulators controlled by Ci-Tbx2/3 is *Fos-a*, a notochord transcription factor that we previously positioned downstream of Ci-Bra (José-Edwards et al., 2011). *Fos-a* appeared among the Ci-Tbx2/3 targets from the microarray analysis of mid-tailbud embryos. Interestingly, *Fos-a* is normally not expressed at the mid-tailbud stage (José-Edwards et al., 2011) and is upregulated in Ci-Tbx2/3^{DBD} transgenics (Table 1), suggesting that it may be repressed by Ci-Tbx2/3. Preliminary *in situ* and qPCR results confirm this result (data not shown). Together, these observations hint at the existence of a transcriptional circuit presided over by Ci-Bra that activates both *Fos-a* and *Ci-Tbx2/3* and is later counterbalanced by Ci-Tbx2/3.

As outlined above, despite the presence of the VP16 activation domain, Ci-Tbx2/3^{VP16} acts also as a dominant-negative form. To verify this point, and to further validate the results of the screens *in vivo*, we looked at the expression of a subset of notochord targets downregulated in embryos expressing *Ci-Tbx2/3^{VP16}* (Fig. 6). Taking advantage of the mosaic incorporation of the transgene, we expected that candidate targets of Ci-Tbx2/3^{VP16}-mediated repression would be absent in notochord cells containing the transgene, but expressed normally in non-transgenic cells. Indeed, we found that *Noto4*, *MLKL*, *ZF105* and *FN1-cont.*, which are normally expressed throughout the notochord in control wild-type embryos (Fig. 6A-D), are detected only in non-transgenic cells in Ci-Tbx2/3^{VP16} embryos (Fig. 6E-H). Accordingly, transgenic notochord cells do not express these genes at detectable levels (Fig. 6E′-H″). These results confirm that, in different contexts, Ci-Tbx2/3^{VP16} can either activate or prevent transcription.

DISCUSSION

A complete understanding of how the developing body plan is shaped requires the reconstruction of the gene circuitry and *cis*-regulatory relationships responsible for cell differentiation in a particular lineage. Through this study, we have identified *Ci-Tbx2/3* as both an effector and a regulator of a wide branch of the gene network downstream of *Ci-Bra* (Fig. 7). The elucidation of numerous Ci-Tbx2/3 targets has allowed us to gain insights into the mechanisms of transcriptional control underlying notochord morphogenesis.

Regulation of *Ci-Tbx2/3* expression in the notochord

We have provided evidence that Ci-Bra is required for the notochord expression of another T-box gene, *Ci-Tbx2/3*. We gathered support for this regulatory relationship from multiple lines of evidence, including the identification of nine T-box binding sites within the *Ci-Tbx2/3* notochord CRM. Detailed examination of the minimal sequences required for the notochord activity of the CRM revealed that the T-box sites function redundantly. The *Ciona intestinalis* genome is highly polymorphic (Dehal et al., 2002), which can lead to faster than usual transcription factor binding site turnover (Satou et al., 2012). The distinctive architecture of the *Ci-Tbx2/3* CRM ensures the precise expression of this transcription

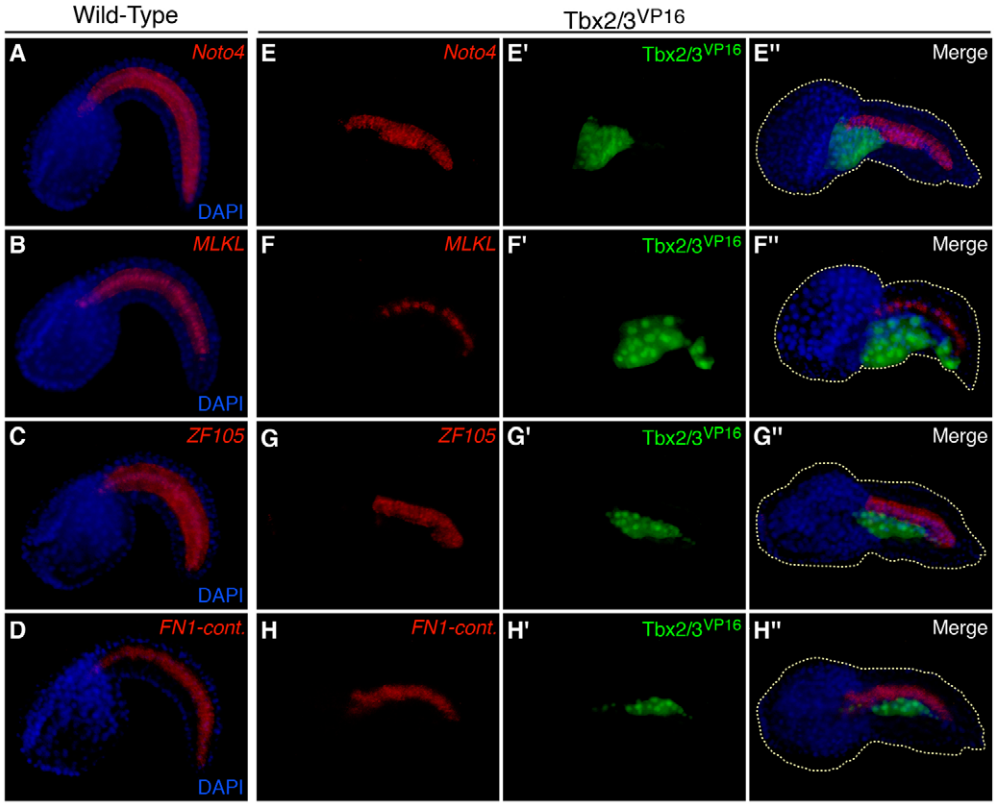

Fig. 6. Ci-Tbx2/3 is required for the expression of notochord genes. (**A-H″**) Fluorescent whole-mount *in situ* hybridization of wild-type (A-D) or *Ci-Tbx2/3^{VP16}::GFP*-expressing (green) embryos (E-H′) with probes (red) for *Noto4* (A,E-E″), *MLKL* (B,F-F″), *ZF105* (C,G-G″) and *FN1-cont.* (D,H-H″), and nuclei counterstained with DAPI (blue). Cont., containing.

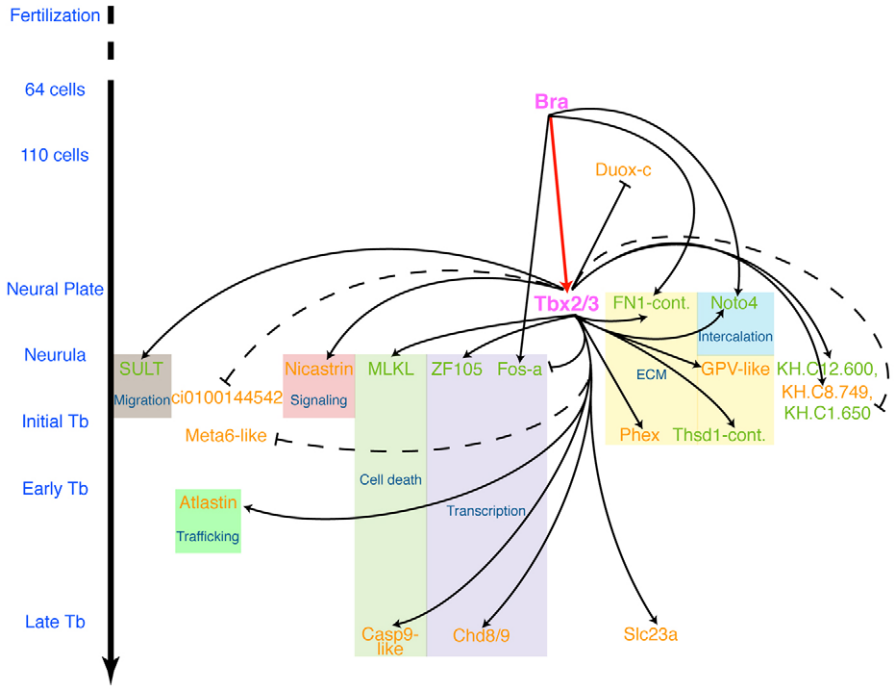

Fig. 7. The notochord gene network downstream of Ci-Bra and Ci-Tbx2/3. The onset of notochord expression of *Ci-Bra*, *Ci-Tbx2/3* and some of the newly identified Ci-Tbx2/3 target genes are plotted against the timeline of *Ciona* developmental stages on the left. Arrows indicate activation of gene expression, whereas bars signify negative regulation. Broken lines are used for those genes that retain weak notochord expression, possibly owing to incomplete repression by Ci-Tbx2/3. Colored boxes encompass genes with similar putative functions. Gene names in green indicate Ci-Tbx2/3-regulated targets that have also been identified as targets of Ci-Bra in previous studies. Names in orange are used for genes that are Ci-Tbx2/3-specific targets. Cont., containing; ECM, extracellular matrix.

factor: the high number and redundancy of T-box sites could counteract the effects of inactivating mutations within its sequence. The ability of the 294 bp construct to direct a similar level of notochord expression in the sister ascidian species *Ciona savignyi* supports this hypothesis. In particular, although the *C. savignyi* sequence is also enriched in T-box sites, these sites often have differing sequences, orientations and spacing than their counterparts in *C. intestinalis*, yet *C. savignyi* embryos retain the ability to properly interpret the *cis*-regulatory information contained in the *C. intestinalis* CRM. This finding hints at a considerable degree of flexibility in the functional requirements of the CRM, which may enable it to sustain changes in its sequence.

Role of Ci-Tbx2/3 in notochord formation and identification of both novel and conserved targets

We showed that upon disruption of Ci-Tbx2/3, CE is greatly impaired by the clustering of transgenic notochord cells that fail to interdigitate into a single row. Consistent with *Ci-Tbx2/3* being a downstream target of Ci-Bra, lack of intercalation was also observed in *Ci-Bra* mutant embryos (Chiba et al., 2009). In other systems, *Tbx2* subfamily genes are expressed in tissues undergoing similar morphogenetic changes. For example, in zebrafish embryos, Tbx2b-deficient ectodermal cells failed to migrate to the neural plate (Fong et al., 2005). Therefore, the ability to coordinate complex cellular movements seems to be an evolutionarily conserved function for these factors.

Through microarray analysis, we uncovered 31 bona fide Ci-Tbx2/3 targets found in its various expression territories, most importantly the notochord. Although leaky activity of the *Ci-Bra* promoter in the mesenchyme (Corbo et al., 1997) could account for some of the genes found in this domain, the transient expression of *Ci-Tbx2/3* in the mesenchyme (Takatori et al., 2004) argues that some of these 18 genes may also represent Ci-Tbx2/3 targets. Nevertheless, among the 31 Ci-Tbx2/3 targets are genes with various putative functions and also genes that are presumably lineage specific, such as *Noto4*. Although lineage specific, Noto4 contains a conserved phosphotyrosine binding domain (PTB) (Yamada et al., 2011). Proteins containing this domain, such as integrins, can bind ECM-contacting proteins (Uhlik et al., 2005). Furthermore, deletion of regions of Noto4 outside of the PTB caused notochord cells to take on a spherical, as opposed to their normally columnar, shape (Yamada et al., 2011), suggesting that Noto4 could also interact with the cytoskeleton and thus affect notochord intercalation through different mechanisms.

A large fraction of Ci-Tbx2/3 targets seem to be involved in the construction and remodeling of the ECM, such as *FN1-cont*. In both the *Xenopus* mesoderm (Davidson et al., 2006) and *Ciona* notochord (Veeman et al., 2008) loss of the ECM components fibronectin and laminin, respectively, results in a lack of CE. Thrombospondin-type 1 domain containing (Thsd1-cont.) proteins mediate cell-cell and cell-matrix interactions in the ECM surrounding the tissues in which they are expressed (Adams, 2001), including the notochord (Urry et al., 1998; Wu et al., 2009). Additionally, extracellular leucine-rich repeat-containing proteins, such as GPV-like, have also been shown to contribute to ECM organization in various animals (Mancuso et al., 2012). The presence of these genes within our list of Ci-Tbx2/3 targets indicates that an analogous loss of ECM integrity could have caused the deficiency of intercalation seen in transgenic embryos. Intercalation is also accomplished through the non-canonical Wnt/planar cell polarity (PCP) pathway. Of note, our results suggested that Ci-Tbx2/3 represses a gene encoding a receptor similar to the LRP canonical Wnt co-receptors (*LRP-like*); it seems conceivable that this could indirectly allow participation of Dsh, a mediator of both non-canonical and canonical/β-catenin Wnt signaling, in PCP at the expense of canonical Wnt signaling to promote notochord cell intercalation.

In vertebrates, the roles of Tbx2/Tbx3 in cancer parallel their functions during embryogenesis. For example, these proteins were recently shown to contribute to epithelial-mesenchymal transition (EMT) (Humtsoe et al., 2012; Wang et al., 2012). Ectopic expression of *TBX2* promoted EMT-like invasiveness of mammary epithelial cells, causing the formation of lamellipodial protrusions

and overexpression of ECM remodelers; both *E-cadherin* and the tight junction protein *ZO1* were also downregulated (Wang et al., 2012). Claudins are another component of tight junctions that help maintain stable contacts between cells (Steed et al., 2010). Interestingly, among the upregulated genes in our screen was *claudin gene family member 3*. Greater notochord cell-cell interactions in embryos where Ci-Tbx2/3 function is impaired could account for the clustering of transgenic notochord cells that we observed. Therefore, overall, cell adhesion and ECM genes appear to be recurrent Tbx2/Tbx3 targets. Notably, although *TBX3* was found to be upregulated in EMT-prone squamous cell carcinoma cells, *DUOX1* was downregulated in a screen for genes differentially expressed in EMT (Humtsoe et al., 2012). Our finding that Ci-Tbx2/3 repressed *Duox-c* in the notochord suggests that TBX3 may similarly regulate the expression of *DUOX1* during EMT. Exploration of the consequences of this relationship that we identified in *Ciona* could thus inform studies of related morphological changes in other biological contexts.

Even though not all *Ciona* genes possess unequivocal vertebrate counterparts, we found parallels with targets identified in previous screens in NIH3T3, ROS17/2.8 (Chen et al., 2001) and HEK293 (Butz et al., 2004) cells overexpressing TBX2. Similarities include targets belonging to the same gene ontology families, such as cytosolic sulfotransferase (SULT), cathepsin and Rgs proteins, and genes involved in ECM formation, cell adhesion and apoptosis. Tail regression of *Ciona* larvae prior to metamorphosis involves apoptosis of various tissues, including those of the notochord, an event involving caspases (Chambon et al., 2002; Nishiyama and Fujiwara, 2008). Although we did not see evidence of apoptosis during tailbud stages, we found that tail resorption in *Ci-Tbx2/3*^{VP16}-expressing larvae was delayed and juveniles retained more tail remnants than wild-type controls (data not shown). Among the notochord genes regulated by Ci-Tbx2/3 was *Caspase9-like* (Fig. 7). Caspases are conserved targets for Tbx2 subfamily members: overexpression of *TBX2* in SW13 adenocarcinoma led to reductions in the activation of caspases 8 and 9 (Ismail and Bateman, 2009). Another Ci-Tbx2/3 notochord target, *MLKL*, was very recently implicated in a mechanism of cell death known as necroptosis (Sun et al., 2012; Zhao et al., 2012); its role in embryonic development remains unclear, but its contribution to notochord morphogenesis can now be investigated using *Ciona* as a model.

Together, these results indicate that *Ci-Tbx2/3* has retained ancestral target genes common to the main chordate lineage and has also acquired control over derived, lineage-specific genes.

The T-box family and the notochord gene regulatory network

The interactions between T-box transcription factors in vertebrates can be exceedingly complex given the large number of family members, many of which are co-expressed. The hierarchical relationship that we identified indicates that, in addition to controlling a specific cohort of genes, Ci-Tbx2/3 serves to both reinforce and refine the Ci-Bra-downstream gene regulatory network. The comparison of Ci-Tbx2/3-regulated genes identified here to those previously classified as Ci-Bra targets suggests that Ci-Bra is required for the initial activation of shared targets that have the same onset as *Ci-Tbx2/3*, such as *Noto4* and *FN1-cont.*, whereas Ci-Tbx2/3 is required to maintain the notochord expression of these genes later in development. Shared targets expressed at later stages of notochord formation may be indirectly regulated by Ci-Bra using Ci-Tbx2/3 as an intermediary, or alternatively Ci-Bra and Ci-Tbx2/3 may cooperatively control expression of these target genes (green font, Fig. 7). By contrast, Ci-Tbx2/3 serves to temporally limit the notochord activity of yet another set of Ci-Bra targets, including *Fos-a*. As noted above, there is also a conspicuous group of Ci-Tbx2/3 targets that do not seem to overlap with those of Ci-Bra (orange font, Fig. 7). These results imply that, despite belonging to the same family and binding similar consensus sequences (Tada and Smith, 2001), T-box transcription factors maintain distinct activities. Consistently, previous work has shown that target specificity is influenced by the DBD itself (Conlon et al., 2001), and it is noteworthy that the T-domains of Ci-Bra and Ci-Tbx2/3 share only 47% identity.

The lack of recognizable activation or repression domains in the Ci-Tbx2/3 protein sequence make its categorization challenging. Nevertheless, the observation that Ci-Tbx2/3 targets are often expressed in a mutually exclusive fashion in the notochord and CNS suggests that Ci-Tbx2/3 works as an activator and is counteracted by localized repressors. However, the similarity of the phenotypes induced by Ci-Tbx2/3^{DBD}, Ci-Tbx2/3^{VP16} and Ci-Tbx2/3^{En}, and the temporal regulation of some of the notochord targets suggest that Ci-Tbx2/3 can ultimately operate as both an activator and a repressor in a context-dependent fashion. This functional duality could depend upon the tissue-specific availability of distinct Ci-Tbx2/3 interacting partners and provides a powerful mechanism that ensures fine-tuned control of tissue identity in the developing embryo.

Acknowledgements

We thank Drs Chiba and Smith (UC Santa Barbara, CA, USA) for providing the *Ci-Bra*$^{-/-}$ embryos.

Funding

This work was supported by the National Institutes of Health/National Institute of General Medical Sciences (NIH/NIGMS) [GM100466] along with supplemental funding from the American Recovery and Reinvestment Act [HD050704-05S1], by the March of Dimes Birth Defects Foundation [1-FY11-468] and by the Charles A. Frueauff Foundation [to A.D.G.]. D.S.J.-E. was supported in part by an NIH training grant [T32 GM008539]. I.O.-I. was supported in part by a fellowship from the Uehara Memorial Foundation (Japan). Research reported in this publication was supported by the National Institute of General Medicine of the NIH. Deposited in PMC for release after 12 months.

Competing interests statement

The authors declare no competing financial interests.

Supplementary material

Supplementary material available online at
http://dev.biologists.org/lookup/suppl/doi:10.1242/dev.094227/-/DC1

References

Adams, J. C. (2001). Thrombospondins: multifunctional regulators of cell interactions. *Annu. Rev. Cell Dev. Biol.* **17**, 25-51.

Butz, N. V., Campbell, C. E. and Gronostajski, R. M. (2004). Differential target gene activation by TBX2 and TBX2VP16: evidence for activation domain-dependent modulation of gene target specificity. *Gene* **342**, 67-76.

Chambon, J.-P., Soule, J., Pomies, P., Fort, P., Sahuquet, A., Alexandre, D., Mangeat, P.-H. and Baghdiguian, S. (2002). Tail regression in Ciona intestinalis (Prochordate) involves a Caspase-dependent apoptosis event associated with ERK activation. *Development* **129**, 3105-3114.

Chen, J., Zhong, Q., Wang, J., Cameron, R. S., Borke, J. L., Isales, C. M. and Bollag, R. J. (2001). Microarray analysis of Tbx2-directed gene expression: a possible role in osteogenesis. *Mol. Cell. Endocrinol.* **177**, 43-54.

Chiba, S., Jiang, D., Satoh, N. and Smith, W. C. (2009). Brachyury null mutant-induced defects in juvenile ascidian endodermal organs. *Development* **136**, 35-39.

Christiaen, L., Davidson, B., Kawashima, T., Powell, W., Nolla, H., Vranizan, K. and Levine, M. (2008). The transcription/migration interface in heart precursors of Ciona intestinalis. *Science* **320**, 1349-1352.

Conlon, F. L., Fairclough, L., Price, B. M., Casey, E. S. and Smith, J. C. (2001). Determinants of T box protein specificity. *Development* **128**, 3749-3758.

Corbo, J. C., Levine, M. and Zeller, R. W. (1997). Characterization of a notochord-specific enhancer from the Brachyury promoter region of the ascidian, Ciona intestinalis. *Development* **124**, 589-602.
Davidson, L. A., Marsden, M., Keller, R. and Desimone, D. W. (2006). Integrin α5β1 and fibronectin regulate polarized cell protrusions required for Xenopus convergence and extension. *Curr. Biol.* **16**, 833-844.
Dehal, P., Satou, Y., Campbell, R. K., Chapman, J., Degnan, B., De Tomaso, A., Davidson, B., Di Gregorio, A., Gelpke, M., Goodstein, D. M. et al. (2002). The draft genome of Ciona intestinalis: insights into chordate and vertebrate origins. *Science* **298**, 2157-2167.
Dheen, T., Sleptsova-Friedrich, I., Xu, Y., Clark, M., Lehrach, H., Gong, Z. and Korzh, V. (1999). Zebrafish tbx-c functions during formation of midline structures. *Development* **126**, 2703-2713.
Di Gregorio, A. and Levine, M. (2002). Analyzing gene regulation in ascidian embryos: new tools for new perspectives. *Differentiation* **70**, 132-139.
Di Gregorio, A., Harland, R. M., Levine, M. and Casey, E. S. (2002). Tail morphogenesis in the ascidian, Ciona intestinalis, requires cooperation between notochord and muscle. *Dev. Biol.* **244**, 385-395.
Dong, B., Horie, T., Denker, E., Kusakabe, T., Tsuda, M., Smith, W. C. and Jiang, D. (2009). Tube formation by complex cellular processes in Ciona intestinalis notochord. *Dev. Biol.* **330**, 237-249.
Dunn, M. P. and Di Gregorio, A. (2009). The evolutionarily conserved leprecan gene: its regulation by Brachyury and its role in the developing Ciona notochord. *Dev. Biol.* **328**, 561-574.
Fong, S. H., Emelyanov, A., Teh, C. and Korzh, V. (2005). Wnt signalling mediated by Tbx2b regulates cell migration during formation of the neural plate. *Development* **132**, 3587-3596.
Frazer, K. A., Pachter, L., Poliakov, A., Rubin, E. M. and Dubchak, I. (2004). VISTA: computational tools for comparative genomics. *Nucleic Acids Res.* **32 Web Server issue**, W273-W279.
Harrelson, Z., Kelly, R. G., Goldin, S. N., Gibson-Brown, J. J., Bollag, R. J., Silver, L. M. and Papaioannou, V. E. (2004). Tbx2 is essential for patterning the atrioventricular canal and for morphogenesis of the outflow tract during heart development. *Development* **131**, 5041-5052.
Herrmann, B. G., Labeit, S., Poustka, A., King, T. R. and Lehrach, H. (1990). Cloning of the T gene required in mesoderm formation in the mouse. *Nature* **343**, 617-622.
Horton, A. C., Mahadevan, N. R., Minguillon, C., Osoegawa, K., Rokhsar, D. S., Ruvinsky, I., de Jong, P. J., Logan, M. P. and Gibson-Brown, J. J. (2008). Conservation of linkage and evolution of developmental function within the Tbx2/3/4/5 subfamily of T-box genes: implications for the origin of vertebrate limbs. *Dev. Genes Evol.* **218**, 613-628.
Hotta, K., Takahashi, H., Asakura, T., Saitoh, B., Takatori, N., Satou, Y. and Satoh, N. (2000). Characterization of Brachyury-downstream notochord genes in the *Ciona intestinalis* embryo. *Dev. Biol.* **224**, 69-80.
Hotta, K., Mitsuhara, K., Takahashi, H., Inaba, K., Oka, K., Gojobori, T. and Ikeo, K. (2007). A web-based interactive developmental table for the ascidian Ciona intestinalis, including 3D real-image embryo reconstructions: I. From fertilized egg to hatching larva. *Dev. Dyn.* **236**, 1790-1805.
Humtsoe, J. O., Koya, E., Pham, E., Aramoto, T., Zuo, J., Ishikawa, T. and Kramer, R. H. (2012). Transcriptional profiling identifies upregulated genes following induction of epithelial-mesenchymal transition in squamous carcinoma cells. *Exp. Cell Res.* **318**, 379-390.
Imai, K. S., Hino, K., Yagi, K., Satoh, N. and Satou, Y. (2004). Gene expression profiles of transcription factors and signaling molecules in the ascidian embryo: towards a comprehensive understanding of gene networks. *Development* **131**, 4047-4058.
Ismail, A. and Bateman, A. (2009). Expression of TBX2 promotes anchorage-independent growth and survival in the p53-negative SW13 adrenocortical carcinoma. *Cancer Lett.* **278**, 230-240.
Jiang, D. and Smith, W. C. (2007). Ascidian notochord morphogenesis. *Dev. Dyn.* **236**, 1748-1757.
Jiang, D., Munro, E. M. and Smith, W. C. (2005). Ascidian prickle regulates both mediolateral and anterior-posterior cell polarity of notochord cells. *Curr. Biol.* **15**, 79-85.
José-Edwards, D. S., Kerner, P., Kugler, J. E., Deng, W., Jiang, D. and Di Gregorio, A. (2011). The identification of transcription factors expressed in the notochord of Ciona intestinalis adds new potential players to the brachyury gene regulatory network. *Dev. Dyn.* **240**, 1793-1805.
Keller, R., Davidson, L., Edlund, A., Elul, T., Ezin, M., Shook, D. and Skoglund, P. (2000). Mechanisms of convergence and extension by cell intercalation. *Philos. Trans. R. Soc. Lond. B Biol. Sci.* **355**, 897-922.
Kubo, A., Suzuki, N., Yuan, X., Nakai, K., Satoh, N., Imai, K. S. and Satou, Y. (2010). Genomic cis-regulatory networks in the early Ciona intestinalis embryo. *Development* **137**, 1613-1623.
Kugler, J. E., Passamaneck, Y. J., Feldman, T. G., Beh, J., Regnier, T. W. and Di Gregorio, A. (2008). Evolutionary conservation of vertebrate notochord genes in the ascidian Ciona intestinalis. *Genesis* **46**, 697-710.
Kusakabe, T., Yoshida, R., Kawakami, I., Kusakabe, R., Mochizuki, Y., Yamada, L., Shin-i, T., Kohara, Y., Satoh, N., Tsuda, M. et al. (2002). Gene expression profiles in tadpole larvae of Ciona intestinalis. *Dev. Biol.* **242**, 188-203.
Lu, J., Li, X.-P., Dong, Q., Kung, H.-F. and He, M.-L. (2010). TBX2 and TBX3: the special value for anticancer drug targets. *Biochim. Biophys. Acta* **1806**, 268-274.
Mancuso, V. P., Parry, J. M., Storer, L., Poggioli, C., Nguyen, K. C. Q., Hall, D. H. and Sundaram, M. V. (2012). Extracellular leucine-rich repeat proteins are required to organize the apical extracellular matrix and maintain epithelial junction integrity in C. elegans. *Development* **139**, 979-990.
Manning, L., Ohyama, K., Saeger, B., Hatano, O., Wilson, S. A., Logan, M. and Placzek, M. (2006). Regional morphogenesis in the hypothalamus: a BMP-Tbx2 pathway coordinates fate and proliferation through Shh downregulation. *Dev. Cell* **11**, 873-885.
Martin, B. L. and Kimelman, D. (2008). Regulation of canonical Wnt signaling by Brachyury is essential for posterior mesoderm formation. *Dev. Cell* **15**, 121-133.
Miwata, K., Chiba, T., Horii, R., Yamada, L., Kubo, A., Miyamura, D., Satoh, N. and Satou, Y. (2006). Systematic analysis of embryonic expression profiles of zinc finger genes in *Ciona intestinalis*. *Dev. Biol.* **292**, 546-554.
Miyamoto, D. M. and Crowther, R. J. (1985). Formation of the notochord in living ascidian embryos. *J. Embryol. Exp. Morphol.* **86**, 1-17.
Munro, E. M. and Odell, G. (2002a). Morphogenetic pattern formation during ascidian notochord formation is regulative and highly robust. *Development* **129**, 1-12.
Munro, E. M. and Odell, G. M. (2002b). Polarized basolateral cell motility underlies invagination and convergent extension of the ascidian notochord. *Development* **129**, 13-24.
Naiche, L. A., Harrelson, Z., Kelly, R. G. and Papaioannou, V. E. (2005). T-box genes in vertebrate development. *Annu. Rev. Genet.* **39**, 219-239.
Nishiyama, A. and Fujiwara, S. (2008). RNA interference by expressing short hairpin RNA in the Ciona intestinalis embryo. *Dev. Growth Differ.* **50**, 521-529.
Oda-Ishii, I. and Di Gregorio, A. (2007). Lineage-independent mosaic expression and regulation of the Ciona multidom gene in the ancestral notochord. *Dev. Dyn.* **236**, 1806-1819.
Packham, E. A. and Brook, J. D. (2003). T-box genes in human disorders. *Hum. Mol. Genet.* **12 Suppl. 1**, R37-R44.
Passamaneck, Y. J. and Di Gregorio, A. (2005). Ciona intestinalis: chordate development made simple. *Dev. Dyn.* **233**, 1-19.
Paxton, C., Zhao, H., Chin, Y., Langner, K. and Reecy, J. (2002). Murine Tbx2 contains domains that activate and repress gene transcription. *Gene* **283**, 117-124.
Sadowski, I., Ma, J., Triezenberg, S. and Ptashne, M. (1988). GAL4-VP16 is an unusually potent transcriptional activator. *Nature* **335**, 563-564.
Satou, Y., Takatori, N., Yamada, L., Mochizuki, Y., Hamaguchi, M., Ishikawa, H., Chiba, S., Imai, K., Kano, S., Murakami, S. D. et al. (2001). Gene expression profiles in Ciona intestinalis tailbud embryos. *Development* **128**, 2893-2904.
Satou, Y., Mineta, K., Ogasawara, M., Sasakura, Y., Shoguchi, E., Ueno, K., Yamada, L., Matsumoto, J., Wasserscheid, J., Dewar, K. et al. (2008). Improved genome assembly and evidence-based global gene model set for the chordate Ciona intestinalis: new insight into intron and operon populations. *Genome Biol.* **9**, R152.
Satou, Y., Shin-i, T., Kohara, Y., Satoh, N. and Chiba, S. (2012). A genomic overview of short genetic variations in a basal chordate, Ciona intestinalis. *BMC Genomics* **13**, 208.
Showell, C., Binder, O. and Conlon, F. L. (2004). T-box genes in early embryogenesis. *Dev. Dyn.* **229**, 201-218.
Steed, E., Balda, M. S. and Matter, K. (2010). Dynamics and functions of tight junctions. *Trends Cell Biol.* **20**, 142-149.
Stemple, D. L. (2005). Structure and function of the notochord: an essential organ for chordate development. *Development* **132**, 2503-2512.
Sun, L., Wang, H., Wang, Z., He, S., Chen, S., Liao, D., Wang, L., Yan, J., Liu, W., Lei, X. et al. (2012). Mixed lineage kinase domain-like protein mediates necrosis signaling downstream of RIP3 kinase. *Cell* **148**, 213-227.
Tada, M. and Smith, J. C. (2001). T-targets: clues to understanding the functions of T-box proteins. *Dev. Growth Differ.* **43**, 1-11.
Takabatake, Y., Takabatake, T. and Takeshima, K. (2000). Conserved and divergent expression of T-box genes Tbx2-Tbx5 in Xenopus. *Mech. Dev.* **91**, 433-437.
Takahashi, H., Hotta, K., Erives, A., Di Gregorio, A., Zeller, R. W., Levine, M. and Satoh, N. (1999). Brachyury downstream notochord differentiation in the ascidian embryo. *Genes Dev.* **13**, 1519-1523.
Takatori, N., Hotta, K., Mochizuki, Y., Satoh, G., Mitani, Y., Satoh, N., Satou, Y. and Takahashi, H. (2004). T-box genes in the ascidian Ciona intestinalis: characterization of cDNAs and spatial expression. *Dev. Dyn.* **230**, 743-753.
Tassy, O., Dauga, D., Daian, F., Sobral, D., Robin, F., Khoueiry, P., Salgado, D., Fox, V., Caillol, D., Schiappa, R. et al. (2010). The ANISEED database: digital representation, formalization, and elucidation of a chordate developmental program. *Genome Res.* **20**, 1459-1468.

Uhlik, M. T., Temple, B., Bencharit, S., Kimple, A. J., Siderovski, D. P. and Johnson, G. L. (2005). Structural and evolutionary division of phosphotyrosine binding (PTB) domains. *J. Mol. Biol.* **345**, 1-20.

Urry, L. A., Whittaker, C. A., Duquette, M., Lawler, J. and DeSimone, D. W. (1998). Thrombospondins in early Xenopus embryos: dynamic patterns of expression suggest diverse roles in nervous system, notochord, and muscle development. *Dev. Dyn.* **211**, 390-407.

Veeman, M. T., Nakatani, Y., Hendrickson, C., Ericson, V., Lin, C. and Smith, W. C. (2008). Chongmague reveals an essential role for laminin-mediated boundary formation in chordate convergence and extension movements. *Development* **135**, 33-41.

Wagner, E. and Levine, M. (2012). FGF signaling establishes the anterior border of the Ciona neural tube. *Development* **139**, 2351-2359.

Wang, B., Lindley, L. E., Fernandez-Vega, V., Rieger, M. E., Sims, A. H. and Briegel, K. J. (2012). The T box transcription factor TBX2 promotes epithelial-mesenchymal transition and invasion of normal and malignant breast epithelial cells. *PLoS ONE* **7**, e41355.

Washkowitz, A. J., Gavrilov, S., Begum, S. and Papaioannou, V. E. (2012). Diverse functional networks of Tbx3 in development and disease. *Wiley Interdiscip. Rev. Syst. Biol. Med.* **4**, 273-283.

Wu, F.-R., Zhou, L.-Y., Nagahama, Y. and Wang, D.-S. (2009). Duplication and distinct expression patterns of two thrombospondin-1 isoforms in teleost fishes. *Gene Expr. Patterns* **9**, 436-443.

Yamada, S., Ueno, N., Satoh, N. and Takahashi, H. (2011). Ciona intestinalis Noto4 contains a phosphotyrosine interaction domain and is involved in the midline intercalation of notochord cells. *Int. J. Dev. Biol.* **55**, 11-18.

Zhao, J., Jitkaew, S., Cai, Z., Choksi, S., Li, Q., Luo, J. and Liu, Z.-G. (2012). Mixed lineage kinase domain-like is a key receptor interacting protein 3 downstream component of TNF-induced necrosis. *Proc. Natl. Acad. Sci. USA* **109**, 5322-5327.